Semiclassical analysis of the weak-coupling limit of SU(2) lattice gauge theory: The extreme infrared region

Jochen Bartels and Bernd Raabe
II. Institut für Theoretische Physik, Universität Hamburg, Hamburg, West Germany

Tai Tsun Wu
Gordon McKay Laboratory, Harvard University, Cambridge, Massachusetts 02138
(Received 23 March 1990)

This paper contains the second part of our systematic investigation of the weak-coupling limit of SU(2) lattice gauge theory, using the semiclassical approximation. We study the flow of solutions close to the subspace of spatially constant fields ("extreme infrared") and establish the existence of a dense cobweb of caustics in the region of very small fields. The origin of these caustics are oscillations of neighboring classical solutions around each other.

I. INTRODUCTION

In a previous paper[1] (henceforth referred to as I) we started a systematic investigation of the weak-coupling limit of SU(2) lattice Yang-Mills[2] theory, using the Hamiltonian formulation and the semiclassical approximation. The first part consisted of a study of classical trajectories in the subspace of spatially constant fields (momentum $\mathbf{k}=0$): They decouple from the other degrees of freedom and can thus be studied separately. In this paper we extend from our analysis and include the modes with $\mathbf{k}\neq 0$. We will, however, restrict ourselves to those trajectories which are close to the $\mathbf{k}=0$ subspace, and we will mainly be interested in the region of very small $\mathbf{k}$. This second part of our study, therefore, deals with the "extreme infrared region." Furthermore, throughout our analysis we shall limit ourselves to the Euclidean region ("classically forbidden region"): This is the region where most of the confinement dynamics is expected to develop.

It will be useful to review a few results of our previous study (I). It has been known for some time[3-7] that the Hamiltonian of the $\mathbf{k}=0$ subspace is nonintegrable; i.e., there is no second integral of motion, and neighboring trajectories depart from each other with a positive Lyapunov exponent. Nevertheless, in this "sea" of irregular (chaotic) classical solutions there exists "islands" which exhibit some regularity. Among these trajectories which emanate from the origin (=point of zero fields) we have found directions where classical trajectories are attracted to each other and oscillate around each other. These oscillations were shown to generate caustics (=set of points where neighboring trajectories intersect with each other). Caustics have the important property that the semiclassical ground-state wave function develops spikes, i.e., potentially may become large. In our case, the caustics were found to start right near the origin, and we have conjectured that they will play an important role in the dynamics of lattice gauge theories in the weak-coupling limit.

In the present paper we continue our study of the flow of the classical lattice Hamiltonian by including the fields with nonzero momentum $\mathbf{k}$. To be more precise, we consider an N^3 lattice model of pure SU(2) Yang-Mills theory with periodic boundary conditions. However, rather than attacking the complete set of coupled nonlinear equations of motion we shall linearize around the solutions of the $\mathbf{k}=0$ sector which we have investigated in paper I. Thus this part of our analysis will be restricted to field configurations which are close to constant fields. Although the main motivation for this restriction is of technical nature [from the highly nonlinear set of equations of motion we split off a zeroth-order part ("unperturbed part") and treat the remainder as a perturbation], this way of progressing towards the full solution is also in accordance with a basic physical argument. In the weak-coupling limit, which defines the continuum limit, we expect that only long-distance phenomena are important, i.e., field configurations with small momenta $\mathbf{k}$.

The main outcome of this paper is that the "focusing" effect which we have observed in the subspace of momenta $\mathbf{k}=0$ remains valid also in the presence of the other degrees of freedom. Namely, the same trajectories of momentum $\mathbf{k}=0$ which were found to attract their neighbors inside the subspace of constant fields do the same also with those of momentum $\mathbf{k}\neq 0$. Such a "parent" trajectory is, therefore, surrounded by oscillating neighbors ("daughters"), and each intersection between them gives rise to caustics. For large N, this "cobweb" of caustics becomes dense and moves close to the origin. The main task of this paper is a careful and detailed study of these oscillations.

Although in this paper we shall not address the question of how this pattern of oscillations in the classical flow translates into dynamical properties of the quantum system, we nevertheless wish to say in a few words why we believe that these oscillations and caustics are important. In Ref. 8 we have discussed in some detail that near a focal point quantum fluctuations around a classical path are stronger than the usual Gaussian fluctuations. For a few examples we have demonstrated how these fluctuations give rise to peaks in the semiclassical wave

function. Strictly speaking, the semiclassical approximation breaks down near a focal point, and the width of the "inaccessible" region (which is, approximately, the same as the width of the peak in the wave function) scales with a certain characteristic positive power of the lattice coupling g^2. It is, however, nevertheless possible to construct the wave function also inside this region, namely, by approximating near the focal point the potential in the Schrödinger equation by a constant, and by requiring that asymptotically the solution match the semiclassical behavior. Caustics, therefore, do not represent a limitation of the semiclassical approximation, but rather signal the onset of genuine quantum behavior, and the semiclassical approximation provides enough information for constructing the wave function. When applying these arguments to the lattice model of this paper, where we find a dense network of caustics close to the origin, we expect that the semiclassical wave function, on a microscopic scale in field space, has many sharp spikes. Looking at these spikes from a larger scale, they are likely to add up to a broader enhancement in the wave function. Some years ago it has been argued by Berry and co-workers[9–11] that the true wave function cannot have such a peaking behavior on an arbitrarily small scale, but has to be smooth over distances (in field space) of the order g^2. The semiclassical wave function, therefore, has to be averaged over distances of this order, before it provides a good approximation to the exact wave function. Conversely, as g^2 becomes smaller and smaller, the true wave function will exhibit more and more of the peaking structure predicted by the semiclassical approximation. If these arguments, which have been verified by numerical calculations so far only for low-dimensional systems in the classically allowed region,[10] also apply to our case, then the ground-state wave function has a very rich fine structure, and more and more of its details will become "visible" in the weak-coupling limit $g^2 \to 0$. This is why we believe that a detailed study of these oscillations (and possibly other sources for caustics) are so significant.

The organization of this paper is the following. In Sec. II we give definitions, specify the lattice Hamiltonian, and write down the equations of motion. We then define the approximation that we are going to use in this paper: We linearize the equations of motion around a parent trajectory which belongs to the subspace of momentum $\mathbf{k}=0$ and has been analyzed in I. In Sec. III we discuss solutions to these equations, in particular the oscillating ones. In Sec. IV we go a little beyond this linear approximation. We show that higher-order corrections make the frequencies depend upon the amplitudes and indicate that this opens the possibility of a much richer resonance structure. We also give the parent trajectory a small component outside the $\mathbf{k}=0$ subspace and study the changes in the accompanying oscillating neighbors. Section V contains a general discussion of the results, and gives an outlook on future steps of this program. A few details of our calculations are put into the Appendix.

II. THE EQUATIONS OF MOTION

We begin with a few definitions which have been made already in I. In our N^3 lattice each site is labeled by a vector $\mathbf{l}$, each link is specified by a site $\mathbf{l}$ and a direction i ($i=1,2,3$), and each plaquette by a site $\mathbf{l}$ and the directions i and j. Link variables belong to the SU(2) gauge group manifold and are parametrized as $U=x_0+i\mathbf{x}\cdot\sigma$ ($x_0^2+\mathbf{x}^2=1$). The lattice Hamiltonian is

$$H=\frac{g^2}{2}\sum_{\text{links}}\mathscr{E}^2(\mathbf{x}_{\mathbf{l},i})+\frac{2}{g^2}\sum_{\text{plaq}}\text{tr}[\mathbb{1}-U(\partial P)]\ , \tag{2.1}$$

where ∂P denotes the boundary of the plaquette P,

$$\mathscr{E}^2(\mathbf{x})=-g^{ab}(\mathbf{x})(\partial_a\partial_b-\Gamma^c_{ab}\partial_c)\ , \tag{2.2}$$

and

$$g^{ab}(\mathbf{x})=\tfrac{1}{4}(\delta_{ab}-x_a x_b)\ . \tag{2.3}$$

We shall work in the approximation $\mathbf{x}^2 \ll 1$. This allows us to drop in Eq. (2.2) the second term with the Christoffel symbols, in Eq. (2.3) the term proportional to $x_a x_b$, and to expand the potential function in powers of $\mathbf{x}^2$. In order to be as close as possible to the continuum theory we shall disregard all terms of higher order than $(\mathbf{x}^2)^2$. A further justification of this approximation will be given below. For the ground-state wave function we make the following ansatz (we limit ourselves to the Euclidean region):

$$\psi(\{\mathbf{x}_{\mathbf{l},i}\})=A\exp\left[-\frac{8}{g^2}S\right]\ , \tag{2.4}$$

where both A and S depend upon the $\mathbf{x}_{\mathbf{l},i}$ and are computed along classical paths. The equations of motion to be solved are of the form

$$\ddot{\mathbf{x}}_{\mathbf{l},i}=\frac{\partial V}{\partial \mathbf{x}_{\mathbf{l},i}}\ . \tag{2.5}$$

The potential function

$$V=\sum_{\mathbf{l},i<j}V_{\mathbf{l},(ij)} \tag{2.6}$$

is a sum over single plaquettes. Each $V_{\mathbf{l},(ij)}$ has the form

$$V_{\mathbf{l},(ij)}=-\tfrac{1}{4}[-\tfrac{1}{2}(\mathbf{x}_1+\mathbf{x}_2-\mathbf{x}_2-\mathbf{x}_4)^2+(\mathbf{x}_2\times\mathbf{x}_3)\cdot\mathbf{x}_4+(\mathbf{x}_3\times\mathbf{x}_4)\cdot\mathbf{x}_1-(\mathbf{x}_4\times\mathbf{x}_1)\cdot\mathbf{x}_2-(\mathbf{x}_1\times\mathbf{x}_2)\cdot\mathbf{x}_3$$
$$+\tfrac{1}{4}(\mathbf{x}_1+\mathbf{x}_2)^2(\mathbf{x}_3+\mathbf{x}_4)^2+\tfrac{1}{4}(\mathbf{x}_1-\mathbf{x}_4)^2(\mathbf{x}_2-\mathbf{x}_3)^2-\tfrac{1}{4}(\mathbf{x}_1+\mathbf{x}_3)^2(\mathbf{x}_2+\mathbf{x}_4)^2-\tfrac{1}{8}(\mathbf{x}_1^2-\mathbf{x}_2^2+\mathbf{x}_3^2-\mathbf{x}_4^2)^2] \tag{2.7}$$

(for simplicity we have set $\mathbf{x}_{\mathbf{l},i}=\mathbf{x}_1$, $\mathbf{x}_{\mathbf{l}+\mathbf{i},j}=\mathbf{x}_2$, $\mathbf{x}_{\mathbf{l}+\mathbf{j},i}=\mathbf{x}_3$, $\mathbf{x}_{\mathbf{l},j}=\mathbf{x}_4$). We introduce the Fourier transform

$$\mathbf{x}_{\mathbf{l},i}=\frac{1}{N^{3/2}}\sum_{\mathbf{k}}e^{i\mathbf{k}\cdot\mathbf{l}}\mathbf{x}_{\mathbf{k},i},\quad \mathbf{p}_{\mathbf{l},i}=\frac{1}{N^{3/2}}\sum_{\mathbf{k}}e^{-i\mathbf{k}\cdot\mathbf{l}}\mathbf{p}_{\mathbf{k},i}\ , \tag{2.8}$$

where $\mathbf{k}=(2\pi/N)(n_1,n_2,n_3)$, and the $\mathbf{p}$'s are the momenta conjugate to the "coordinates" $\mathbf{x}$'s. With this we go into Eqs. (2.6) and (2.7). We will be interested in the region of small momenta and expand in powers of $\mathbf{k}$. The potential function V then becomes

$$V=\frac{1}{4}\left[\frac{1}{2}\sum_{\mathbf{k}}\mathbf{x}_{-\mathbf{k},i}(\mathbf{k}^2\delta_{ij}-k_ik_j)\mathbf{x}_{\mathbf{k},j}+2i\frac{1}{N^{3/2}}\sum_{\{\mathbf{k}\}}\delta(\mathbf{k}_1+\mathbf{k}_2+\mathbf{k}_3)k_{1i}\epsilon^{abc}x^a_{k_1 j}x^b_{k_2 j}x^c_{k_3 i}\right.$$
$$\left.+\frac{1}{N^3}\sum_{\{\mathbf{k}\}}\delta(\mathbf{k}_1+\mathbf{k}_2+\mathbf{k}_3+\mathbf{k}_4)\epsilon^{abm}\epsilon^{cdm}x^a_{k_1 i}x^c_{k_2 i}x^b_{k_3 j}x^d_{k_4 j}\right] . \tag{2.9}$$

For later convenience we rescale all $\mathbf{p}$'s and $\mathbf{x}$'s by $1/N^{3/2}$: in the equations of motion (2.5) then all factors of N drop out.

It is easily seen that the solutions with $\mathbf{k}=0$ decouple: Setting $\mathbf{x}_{\mathbf{k},i}=0$ for all $\mathbf{k}\neq 0$, the equations of motion Eq. (2.5) reduce to a set of nine coupled equations. Because of rotational symmetry in group space (global gauge invariance) and in ordinary space, they can be further reduced down to three equations. The study of these three equations was the content of I. Two solutions were found to be of special interest:

$$\mathbf{x}_{0,1}=\frac{\sqrt{2}}{-t}\begin{bmatrix}1\\0\\0\end{bmatrix},\quad \mathbf{x}_{0,2}=\frac{\sqrt{2}}{-t}\begin{bmatrix}0\\1\\0\end{bmatrix},$$
$$\mathbf{x}_{0,3}=\begin{bmatrix}0\\0\\0\end{bmatrix} \tag{2.10}$$

and

$$\mathbf{x}_{0,1}=\frac{1}{-t}\begin{bmatrix}1\\0\\0\end{bmatrix},\quad \mathbf{x}_{0,2}=\frac{1}{-t}\begin{bmatrix}0\\1\\0\end{bmatrix},$$
$$\mathbf{x}_{0,3}=\frac{1}{-t}\begin{bmatrix}0\\0\\1\end{bmatrix} \tag{2.11}$$

(and their rotated counterparts in group or ordinary space). For the first solution (2.10) we have found that it is surrounded by oscillating neighboring trajectories, and the caustics which they generate form nested cones. The second solution (2.11) has no such oscillations, but it is the line where all the cones around (2.10) intersect with each other.

In this paper we want to turn on the degrees of freedom with momentum $\mathbf{k}\neq 0$, but we still do not want to go too far away from the subspace $\mathbf{k}=0$. We are searching for solutions of the form

$$\mathbf{x}_{\mathbf{k},i}(t)=\mathbf{y}_i(t)+\delta\mathbf{x}_{\mathbf{k},i}(t) , \tag{2.12}$$

where $\mathbf{y}_i=\mathbf{x}_{0,i}$ is given by either (2.10) or (2.11) and

$$|\delta\mathbf{x}_{\mathbf{k},i}(t)|\ll|\mathbf{y}_i(t)| . \tag{2.13}$$

In the following we will use the notation $\mathbf{x}_{\mathbf{k},i}$ for $\delta\mathbf{x}_{\mathbf{k},i}$. For the small deviations $\mathbf{x}_{\mathbf{k},i}$ the equations of motion become linear. If we introduce the nine-component vector

$$X_{\mathbf{k}}=\begin{bmatrix}\mathbf{x}_{\mathbf{k},1}\\\mathbf{x}_{\mathbf{k},2}\\\mathbf{x}_{\mathbf{k},3}\end{bmatrix} , \tag{2.14}$$

the linearized equations of motion are conveniently written in form of a matrix equation

$$\ddot{X}_{\mathbf{k}}(t)=[A+iB(t)+C(t)]X_{\mathbf{k}}(t)+O(X^2) . \tag{2.15}$$

A,B,C are 9×9 matrices. The matrix A is independent of $\mathbf{y}$ and quadratic in $\mathbf{k}$, B is linear in both $\mathbf{y}$ and $\mathbf{k}$, and C is quadratic in $\mathbf{y}$ and independent of $\mathbf{k}$. In more detail, the matrices A,B,C consist of 3×3 block matrices, and we denote the elements of $A_{(ia),(bj)}$ (i and j refer to spatial directions, a and b to directions in group space). We then have

$$A_{(ia),(jb)}=\frac{1}{4}(\delta_{ij}\mathbf{k}^2-k_ik_j)\delta^{ab} , \tag{2.16}$$

$$B_{(ia),(jb)}=[-k_l y^c_l\delta_{ij}+\frac{1}{2}(k_i y^c_j+k_j y^c_i)]\epsilon^{abc} , \tag{2.17}$$

$$C_{(ia),(jb)}=\sum_l(\delta^{ab}\mathbf{y}_l^2-y^a_l y^b_l)\delta_{ij}$$
$$-(\delta^{ab}\mathbf{y}_i\cdot\mathbf{y}_j-y^a_i y^b_j)+\epsilon^{abc}(\mathbf{y}_i\times\mathbf{y}_j)^c . \tag{2.18}$$

Equation (2.15) [with Eqs. (2.14) and (2.16)–(2.18)] is an approximation to the full set of equations of motion (2.5). Its validity is restricted by the constraints

$$0\le|\mathbf{x}_{\mathbf{k}i}|\ll|\mathbf{y}_i|=O(1/|t|)\ll 1 ,$$
$$0<|\mathbf{k}|\ll 1 . \tag{2.19}$$

There are two special cases of these conditions, where the equations of motion become particularly simple

$$\frac{1}{|t|}\sim|\mathbf{y}_i|\ll|\mathbf{k}_i|\ll 1 \tag{2.20}$$

and

$$|\mathbf{k}|\ll|\mathbf{y}_i|\sim\frac{1}{|t|}\ll 1 . \tag{2.21}$$

In the first case we can drop the two terms B and C. This is the region where ordinary perturbation theory around the zero-field point works. For the second case (2.21) the terms proportional to A and B are small compared to the third one. We are interested in regions where the terms B (triple-gluon coupling) and C (quartic-gluon coupling) have nontrivial effects, and (2.21) is an extreme case of this.

Finally we have to say a few words about the question

of gauge fixing. In order to keep the equations of motion as simple as possible, we choose, in this paper, to work without any gauge fixing. Any such constraint would inevitably make the kinetic part of the Hamiltonian nonlocal and thus spoil the simple form of the equations of motion. The obvious disadvantage of this, on the other hand, lies in the fact that the space of field configurations is larger than really necessary. For each classical trajectory there are neighboring solutions which are merely images under infinitesimal gauge transformations. Generators of these symmetry transformations are constants of motion:

$$G_1^a=\sum_{i=1}^{3}[(x_{1,i}^0\mathbf{p}_{1,i}-x_{1-i,i}^0\mathbf{p}_{1-i,i})^a -(\mathbf{x}_{1,i}\times\mathbf{p}_{1,i})^a-(\mathbf{x}_{1-i,i}\times\mathbf{p}_{1-i,i})^a] \tag{2.22}$$

[here $\mathbf{p}_{1,i}$ are the momenta canonically conjugate to the coordinates $\mathbf{x}_{1,i}$, and we are returning to the notation used in and after Eq. (2.1)]. In the approximation $|\mathbf{x}_{1,i}|\ll 1$ and $|\mathbf{p}_{1,i}|\ll 1$ (2.22) becomes

$$G_1^a=\sum_{i=1}^{3}[(\mathbf{p}_{1,i}-\mathbf{p}_{1-i,i})^a-(\mathbf{x}_{1,i}\times\mathbf{p}_{1,i})^a-(\mathbf{x}_{1-i,i}\times\mathbf{p}_{1-i,i})^a] \tag{2.23}$$

and the infinitesimal gauge transformations are

$$\delta\mathbf{x}_{1,i}=\mathbf{g}_1-\mathbf{g}_{1+i}+\mathbf{x}_{1,i}\times(\mathbf{g}_1+\mathbf{g}_{1+i})\ , \tag{2.24}$$

$$\delta\mathbf{p}_{1,i}=\mathbf{p}_{1,i}\times(\mathbf{g}_1+\mathbf{g}_{1+i})\ . \tag{2.25}$$

In the following we will discuss small deviations away from the parent trajectories (2.10) or (2.11). It will be important to distinguish between those directions away from the parent trajectory which are obtained by the canonical transformations (2.24) and (2.25) and hence are the gauge images, and others which lead to new and independent classical solutions.

III. SOLUTIONS TO THE LINEARIZED EQUATIONS OF MOTION

We begin with by investigating the vicinity of the solution (2.10). With $t=2\tau$ and $\mathbf{k}=(k_1,k_2,k_3)$ the linearized equations of motion become

$$\frac{d^2X}{d\tau^2}=\left[A+i\frac{\sqrt{2}}{\tau}B+\frac{2}{\tau^2}C\right]X\ . \tag{3.1}$$

The explicit form of the 9×9 matrices A,B,C is

$$A=\begin{bmatrix}(k_2^2+k_3^2)\mathbb{1} & -k_1k_2\mathbb{1} & -k_1k_3\mathbb{1}\\ -k_1k_2\mathbb{1} & (k_1^2+k_3^2)\mathbb{1} & -k_2k_3\mathbb{1}\\ -k_1k_3\mathbb{1} & -k_2k_3\mathbb{1} & (k_1^2+k_2^2)\mathbb{1}\end{bmatrix}, \tag{3.2}$$

where we have used block matrix notation,

$$B=\begin{bmatrix}
 & 2k_2 & & -k_1 & & & & & \\
 & & & k_2 & & & & & k_3\\
-2k_2 & & & k_1 & -k_2 & & & -k_3 & \\
 & & -k_1 & & & & & & -k_3\\
 & & k_2 & & & -2k_1 & & & \\
k_1 & -k_2 & & & 2k_1 & & k_3 & & \\
 & & & & & -k_3 & & & 2k_2\\
 & & k_3 & & & & & & -2k_1\\
 & -k_3 & & k_3 & & & -2k_2 & 2k_1 &
\end{bmatrix} \tag{3.3}$$

and

$$C=\begin{bmatrix}
1 & & & & 2 & & & & \\
 & 0 & & -1 & & & & & \\
 & & 1 & & & & & & \\
 & -1 & & 0 & & & & & \\
2 & & & & 1 & & & & \\
 & & & & & 1 & & & \\
 & & & & & & 1 & & \\
 & & & & & & & 1 & \\
 & & & & & & & & 2
\end{bmatrix}. \tag{3.4}$$

It is not possible to diagonalize all these matrices simultaneously. The commutators of A and B or B and C are zero only for $\mathbf{k}=\mathbf{0}$, whereas $[A,C]=0$ for $\mathbf{k}=(0,0,k)$. We, therefore, concentrate on this simplest case and we shall come back to the more general case somewhat later. Introducing in (3.1) the new time variable $k\tau$ instead of τ we find for A and B the simpler expressions

$$A=\begin{bmatrix}
1 & & & & & & & & \\
 & 1 & & & & & & & \\
 & & 1 & & & & & & \\
 & & & 1 & & & & & \\
 & & & & 1 & & & & \\
 & & & & & 1 & & & \\
 & & & & & & 0 & & \\
 & & & & & & & 0 & \\
 & & & & & & & & 0
\end{bmatrix}, \tag{3.5}$$

$$B=\begin{bmatrix} 0 & & & & & & 0 & 0 & 0 \\ & 0 & & & & & 0 & 0 & 1 \\ & & 0 & & & & 0 & -1 & 0 \\ & & & 0 & & & & & -1 \\ & & & & 0 & & & & \\ & & & & & 0 & 1 & & \\ 0 & 0 & 0 & & & -1 & 0 & & \\ 0 & 0 & 1 & & & & & 0 & \\ 0 & -1 & 0 & 1 & & & & & 0 \end{bmatrix} \tag{3.6}$$

(C does not depend upon k and therefore remains unchanged). A and B are easily brought into diagonal form through two rotations in the 1-5 plane and in the 2-4 plane by 45°. The matrix A is the same as before, but B and C have changed into

$$B=\begin{bmatrix} 0 & & & & & & 0 & 0 & 0 \\ & 0 & & & & & 0 & 0 & 0 \\ & & 0 & & & & 0 & -1 & 0 \\ & & & 0 & & & & & -\sqrt{2} \\ & & & & 0 & & & & \\ & & & & & 0 & 1 & & \\ 0 & 0 & 0 & & & -1 & 0 & & \\ 0 & 0 & 1 & & & & & 0 & \\ 0 & 0 & 0 & \sqrt{2} & & & & & 0 \end{bmatrix}, \tag{3.7}$$

$$C=\begin{bmatrix} 3 & & & & & & & & \\ & -1 & & & & & & & \\ & & 1 & & & & & & \\ & & & 1 & & & & & \\ & & & & -1 & & & & \\ & & & & & 1 & & & \\ & & & & & & 1 & & \\ & & & & & & & 1 & \\ & & & & & & & & 2 \end{bmatrix}. \tag{3.8}$$

The nine differential equations (3.1) now decouple into five separate sets of equations.

Case (1) (lines 2 or 5)

$$\frac{d^2x}{d\tau^2}=\left[1-\frac{2}{\tau^2}\right]x\ . \tag{3.9}$$

Case (2) (line 1)

$$\frac{d^2x}{d\tau^2}=\left[1+\frac{6}{\tau^2}\right]x\ . \tag{3.10}$$

Case (3) (lines 3 and 8; lines 6 and 7 are the complex conjugates)

$$\frac{d^2x}{d\tau^2}=\left[\begin{bmatrix}1&0\\0&0\end{bmatrix}+\frac{i\sqrt{2}}{\tau}\begin{bmatrix}0&-1\\1&0\end{bmatrix}+\frac{2}{\tau^2}\begin{bmatrix}1&0\\0&1\end{bmatrix}\right]x\ . \tag{3.11}$$

Case (4) (lines 4 and 9)

$$\frac{d^2x}{d\tau^2}=\left[\begin{bmatrix}1&0\\0&0\end{bmatrix}+\frac{i\sqrt{2}}{\tau}\begin{bmatrix}0&-\sqrt{2}\\\sqrt{2}&0\end{bmatrix}+\frac{2}{\tau^2}\begin{bmatrix}1&0\\0&2\end{bmatrix}\right]x\ . \tag{3.12}$$

We are looking for solutions which, in the infinite past, leave from the origin. They all can be expressed in terms of elementary functions or, at most, integrals over elementary functions. Cases (1) and (2) are Bessel equations

$$(1)\quad x(\tau)=\text{const}\times\sqrt{-\tau}K_{i\omega}(-\tau),\quad \omega=\tfrac{1}{2}\sqrt{7}\ , \tag{3.13}$$

$$(2)\quad x(\tau)=\text{const}\times\sqrt{-\tau}K_{5/2}(-\tau)\ . \tag{3.14}$$

Case (3) is solved as follows. Denote the two components by x_1 and x_2. From the first line one obtains $x_2=(i\tau/\sqrt{2})[x_1''-x_1-(2/\tau^2)x_1]$ and substitutes into the second line:

$$\tau^3x_1''''+2\tau^2x_1'''-(\tau^3+4\tau)x_1''-2(\tau^2-2)x_1'=0\ . \tag{3.15}$$

Set $x_1'=u/\tau^2$

$$\tau^2u'''-4\tau u''+(6-\tau^2)u'=0\ . \tag{3.16}$$

Finally, with $u'=v\tau^2$,

$$v''-v=0\ . \tag{3.17}$$

We chose the solution which goes to zero as $\tau\to-\infty$

$$u=Ce^{\tau}\ . \tag{3.18}$$

This gives, after a few partial integrations,

$$x_1(\tau)=C\left[\frac{1}{2}+\frac{1}{-\tau}\right]e^{\tau}\ , \tag{3.19}$$

$$x_2(\tau)=C\frac{i}{\sqrt{2}\tau}e^{\tau}\ . \tag{3.20}$$

Case (4) is treated in a similar way. From the second line one obtains $x_1=-i\tau[\frac{1}{2}x_2''-(2/\tau^2)x_2]$. We insert this into the first line

$$x_2''''+\left[\frac{2}{\tau}x_2'''-\frac{2}{\tau^2}x_2''\right]-\left[\frac{4}{\tau^2}x_2''-\frac{8}{\tau^3}x_2'\right]-x_2''=0 \tag{3.21}$$

or

$$\frac{d}{d\tau}\frac{1}{\tau}\left[(\tau x_2')'-\left[1+\frac{4}{\tau^2}\right]\tau x_2'\right]=0\ . \tag{3.22}$$

This can easily be integrated, and with $u=\tau x_2'$ we obtain

$$u''-\left[1+\frac{4}{\tau^2}\right]u=C\tau\ . \tag{3.23}$$

Here C is a constant which will be shown to be zero for our case. The solution to the homogeneous equation with the correct behavior for $\tau\to\infty$ is

$$u_1(\tau)=\sqrt{-\tau}K_{\sqrt{17}/2}(-\tau)\ . \tag{3.24}$$

A particular solution to the inhomogeneous equations is found as

$$u_{\text{inhom}}(\tau)=\frac{C}{W}\left[u_2(\tau)\int_{-\infty}^{\tau}d\tau' u_1(\tau')\tau' + u_1(\tau)\int_{\tau}^{0}d\tau' u_2(\tau')\tau'\right], \tag{3.25}$$

where u_1 is given in (3.24),

$$u_2(\tau)=\sqrt{-\tau}I_{\sqrt{17}/2}(-\tau) \tag{3.26}$$

and $W=-1$. For $\tau\to-\infty$, $u_{\text{inhom}}(\tau)$ increases as $\sim C\tau$, and this cannot be compensated by adding any solution of the homogeneous equation. So $u(\tau)\sim C\tau$ and also $x_2\sim C\tau$, unless $C=0$. This then leaves us with (3.24) for $u(\tau)$. Returning to x_1 and x_2, we find

$$x_1(\tau)=\frac{iC'}{-2\tau}\int_{-\infty}^{\tau}d\tau'\sqrt{-\tau'^3}K_{\sqrt{17}/2}(-\tau'), \tag{3.27}$$

$$x_2(\tau)=C'\int_{-\infty}^{\tau}\frac{d\tau'}{\sqrt{-\tau'}}K_{\sqrt{17}/2}(-\tau'). \tag{3.28}$$

Let us discuss a few aspects of these solutions. For $\tau\to-\infty$ [region (2.20) with $-1/t\ll|k|$] all solutions go to zero exponentially, as it is predicted by perturbation theory. More interesting is the behavior for small τ, i.e., $|k|\ll-1/t\ll1$ [region (2.21)]. This is the region where in the differential equation (3.1) we can disregard the first two terms, and all essential information is contained in the eigenvalues of the matrix C [Eq. (3.8)]. The negative ones signal attraction to the parent trajectory,

$$x(\tau)\sim\sqrt{-\tau}\cos\left[\omega\ln\left[\frac{-\tau}{2}\right]-\phi_0\right], \tag{3.29}$$

whereas the positive ones indicate repulsion

$$x(\tau)\sim(-\tau)^{-p} \tag{3.30}$$

with $p=2$, 1, $(\sqrt{17}-1)/2$ for the eigenvalues 3, 1, 2, respectively. One easily verifies that (3.13), (3.14), (3.19) and (3.20), and (3.27) and (3.28) have, in fact, this asymptotic behavior for $\tau\to0$.

The oscillating trajectories (3.13) [or (3.29)] are the most interesting ones, since they produce caustics. The frequency ω and the strength of the "friction" are the same for all values of k. Consider the solution (3.13) and its dependence upon the momentum k. Since for small values of its argument the Bessel function goes as

$$K_{i\omega}(z)=\rho\cos\left[\omega\ln\frac{z}{2}-\phi_0\right][1+O(z^2)] \tag{3.31}$$

with

$$\Gamma(i\omega)=\rho e^{i\phi_0},$$
$$\rho^2=\frac{\pi}{\omega\sinh(\pi\omega)}, \tag{3.32}$$
$$\phi_0=\lim_{n\to\infty}\left[\omega\ln n-\frac{\pi}{2}-\sum_{k=1}^{n-1}\arctan\left[\frac{\omega}{k}\right]\right],$$

there will be an infinite sequence of positive zeros of $K_{i\omega}(z)$, which accumulate at zero

$$z_1>z_2>\cdots>z_n>z_{n+1}>\cdots>0. \tag{3.33}$$

For sufficiently large n, $z_n/z_{n+1}=\exp(\pi/\omega)$. Following the parent trajectory which at $t=-\infty$ starts at the origin, the first intersection will be with the oscillating trajectory of smallest k, $k_{\min}$. This will be at time

$$-t_1=\frac{4z_1}{k_{\min}}. \tag{3.34}$$

Subsequent intersections with the same trajectory occur at times

$$-t_2=\frac{4z_2}{k_{\min}},\quad -t_3=\frac{4z_3}{k_{\min}},\ldots, \tag{3.35}$$

$$\frac{t_n}{t_{n+1}}\approx\exp(\pi/\omega). \tag{3.36}$$

A similar string of intersection points belongs to any other k value. For sufficiently large N (=size of the lattice) the smallest nonzero value k is arbitrarily small, and the sequence of focal points along the parent trajectory becomes arbitrarily dense. This is one of the main results of this paper.

What about the other, nonoscillating directions? As we have discussed at the end of Sec. III, there must be some directions which belong to local gauge transformations. Translating (2.24) and (2.25) into Fourier space and applying it to our parent trajectory (2.10), we find that for each momentum $\mathbf{k}$ there must be three different gauge copies under infinitesimal gauge transformations. For $\mathbf{k}=(0,0,k)$ they are

$$\delta\mathbf{x}_{\mathbf{k},1}=\begin{bmatrix}0\\0\\0\end{bmatrix},\quad \delta\mathbf{x}_{\mathbf{k},2}=-\frac{2\sqrt{2}}{t}\begin{bmatrix}0\\0\\1\end{bmatrix},$$
$$\delta\mathbf{x}_{\mathbf{k},3}=-ik\begin{bmatrix}1\\0\\0\end{bmatrix}, \tag{3.37}$$

and

$$\delta\mathbf{x}_{\mathbf{k},1}=-\frac{2\sqrt{2}}{t}\begin{bmatrix}0\\0\\1\end{bmatrix},\quad \delta\mathbf{x}_{\mathbf{k},2}=\begin{bmatrix}0\\0\\0\end{bmatrix},$$
$$\delta\mathbf{x}_{\mathbf{k},3}=-ik\begin{bmatrix}0\\1\\0\end{bmatrix}, \tag{3.38}$$

and

$$\delta\mathbf{x}_{\mathbf{k},1}=-\frac{2\sqrt{2}}{t}\begin{bmatrix}0\\1\\0\end{bmatrix},\quad \delta\mathbf{x}_{\mathbf{k},2}=\frac{2\sqrt{2}}{t}\begin{bmatrix}1\\0\\0\end{bmatrix},$$
$$\delta\mathbf{x}_{\mathbf{k},3}=-ik\begin{bmatrix}0\\0\\1\end{bmatrix}. \tag{3.39}$$

One can check that they are, in fact, solutions to the equations of motion (3.1). From this we conclude, in particular, that the oscillating solutions which we have discussed before reflect genuine dynamical effects, rather

than simply being gauge artifacts.

Next we want the momentum vector $\mathbf{k}$ to be more general than $(0,0,k)$. For such general $\mathbf{k}$ we have not been able to find solutions which can be expressed in terms of elementary functions. Fortunately, however, the most important information on the existence of oscillations resides in the matrix C, the third term of the differential equation (3.1), which is independent of momentum $\mathbf{k}$. It is then sufficient to verify the existence of solutions which for $t\to-\infty$ are exponentially small, and for $\tau\to 0$ turn into such an oscillating solution. This we have checked with a computer: We have followed the first zero z_1 as a function of the direction of the vector $\mathbf{k}$ (keeping the magnitude of $\mathbf{k}$ fixed). When $\mathbf{k}$ leaves the three-direction, the degeneracy of the two oscillating solutions is lifted, and the zero breaks up into a pair of zeros which slowly start to move towards the origin (the closest distance from the origin is reached when $\mathbf{k}$ is orthogonal to the three-direction). This shows that the situation changes continuously when $\mathbf{k}$ changes direction, and the existence of oscillating solutions holds for arbitrary directions of $\mathbf{k}$.

Before ending this section we look into the vicinity of the other parent trajectory (2.11). In accordance with our findings in I we shall show that, from the point of view of caustics, this trajectory is much more difficult to study than the previous case. As we have learned before, the essential information on the motion of neighboring trajectories is contained in the eigenvalues of the matrix C. We, therefore, substitute (2.11) into the general expression for C [Eq. (2.18)] and obtain [again for $\mathbf{k}=(0,0,k)$]

$$C=\begin{pmatrix} 2 & & & & 2 & & & & 2 \\ & 1 & & -1 & & & & & \\ & & 1 & & & & -1 & & \\ & -1 & & 1 & & & & & \\ 2 & & & & 2 & & & & 2 \\ & & & & & 1 & & -1 & \\ & & -1 & & 0 & & 1 & & \\ & & & & & -1 & & 1 & \\ 2 & & & & 2 & & & & 2 \end{pmatrix} . \tag{3.40}$$

Its eigenvalues are found to be 6,2,2,2,0,0,0,0,0,0, i.e., there is no negative one. For $\tau\to 0$ the solutions go as $(-\tau)^{-p}$ with $p=2,1,1,1,0,0,0,0,0,0$, respectively. Our study of the linearized equations of motion, therefore, seems to indicate that there are no caustics in the vicinity of this trajectory. However, our numerical analysis described in I has told us that, in the $\mathbf{k}=0$ subspace, this ray is the intersection of infinitely many caustic cones. This could not be seen by studying the linearized equations of motion but only by numerically following the caustic surfaces. A similar situation might also hold for the $\mathbf{k}\neq 0$ directions. Either further computer studies or more advanced analytic methods are needed to find a reliable answer.

It may be of interest to note that, at least initially, this trajectory (2.11) coincides with the instanton solution.[12] In the $A_0=0$ gauge the instanton has the form[13]

$$\mathbf{A}_k=U^{-1}(\overline{\mathbf{A}}_k+\partial_k)U \tag{3.41}$$

with

$$\overline{\mathbf{A}}_k=\frac{-i}{x^2+\lambda^2}(x_0\sigma_k+\epsilon_{kml}x_m\sigma_l) , \tag{3.42}$$

$$\overline{A}_0=i\frac{\mathbf{x}\sigma}{x^2+\lambda^2} , \tag{3.43}$$

$$U=T\exp\left[-\int^t dt'\,\overline{A}_0(\mathbf{x},t')\right]$$

$$=\cos\phi+i\frac{\boldsymbol{\sigma}\cdot\mathbf{x}}{|\mathbf{x}|}\sin\phi , \tag{3.44}$$

$$\phi=\frac{|\mathbf{x}|}{\sqrt{\mathbf{x}^2+\lambda^2}}\arctan\left[\frac{\sqrt{\mathbf{x}^2+\lambda^2}}{-t}\right] . \tag{3.45}$$

For $t\to-\infty$

$$\mathbf{A}_k=-\frac{2i\lambda^2}{3t^3}\sigma_k+O(t^{-5}) , \tag{3.46}$$

i.e., $\mathbf{A}_k$ is proportional to the parent trajectory (2.11). This explains why one would not expect to see caustics when linearizing the equations of motion around the instanton solution, and the calculation of Gaussian fluctuations around the instanton in the path integral does not lead to any difficulties. It follows, however, from what we have said before that in fact the situation may be much more complicated and the linear approximation is insufficient to extract the correct structure near the instanton paths.

IV. HIGHER-ORDER CORRECTIONS

So far our discussion has been restricted to the linear approximation of the equations of motion around the two parent trajectories (2.10) and (2.11). In this section we discuss a few effects of the nonlinear terms in (2.15) [denoted by $O(X^2)$] around the trajectory (2.10). Of particular interest are the oscillating solutions. One of the peculiar features that we encountered in the linear approximation was the fact that the frequencies were the same for all momenta k. Will this degeneracy be lifted once we include higher-order corrections? For simplicity we will again restrict ourselves to the case $\mathbf{k}=(0,0,k)$. In this case we can make use of the analytic solutions found in Sec. III. Furthermore we have, in addition to the gauge symmetry, also symmetry of spatial rotations around the direction of $\mathbf{k}$ vector, i.e., in the 1-2 plane.

To simplify calculations, it is convenient to use the following 3×3 matrix notation:

$$X_{\mathbf{k}}=(\mathbf{x}_{\mathbf{k},1}(t),\mathbf{x}_{\mathbf{k},2}(t),\mathbf{x}_{\mathbf{k},3}(t)) . \tag{4.1}$$

In this notation our parent trajectory (2.10) has the form

$$Y(t)=\frac{\sqrt{2}}{-t}\begin{pmatrix} 1 & 0 & 0 \\ 0 & 1 & 0 \\ 0 & 0 & 0 \end{pmatrix} . \tag{4.2}$$

The oscillating solutions found in the previous section have the structure

$$X_{\mathbf{k}}=\text{const}\times\sqrt{-\tau}K_{i\omega}(-\tau)\begin{bmatrix}1&0&0\\0&-1&0\\0&0&0\end{bmatrix} \tag{4.3}$$

or

$$X_{\mathbf{k}}=\text{const}\times\sqrt{-\tau}K_{i\omega}(-\tau)\begin{bmatrix}0&1&0\\1&0&0\\0&0&0\end{bmatrix}. \tag{4.4}$$

Since the latter form can always be diagonalized through gauge rotations or spatial rotations, it is sufficient to consider only the first case. A closer inspection of the potential function (2.9) shows that the following ansatz leads to a closed system of equations of motion

$$X_k=f_k(t)\begin{bmatrix}1&0&0\\0&1&0\\0&0&0\end{bmatrix}+g_k(t)\begin{bmatrix}1&0&0\\0&-1&0\\0&0&0\end{bmatrix}. \tag{4.5}$$

The equations of motion are

$$\left[\frac{d^2}{dt^2}-\frac{k^2}{4}\right]f_k=\sum_{\{k\}}f_{k_1}f_{k_2}f_{k_3}-\sum_{\{k\}}g_{k_1}g_{k_2}f_{k_3}\,, \tag{4.6}$$

$$\left[\frac{d^2}{dt^2}-\frac{k^2}{4}\right]g_k=\sum_{\{k\}}g_{k_1}g_{k_2}g_{k_3}-\sum_{\{k\}}f_{k_1}f_{k_2}g_{k_3}\,. \tag{4.7}$$

Here the summation includes momentum conservation $k_1+k_2+k_3+k=0$. [As a side remark we note that these equations represent the equations of motion of the lattice version of the Lagrangian of a two-component (Euclidean) field theory in $1+1$ dimensions

$$L=\tfrac{1}{2}(\partial_t\phi_i)^2+\tfrac{1}{2}m^2(\partial_z\phi_i)^2+\tfrac{1}{4}(\phi_1^2-\phi_2)^2 \tag{4.8}$$

with $m^2=\frac{1}{4}$.]

The equations of motion (4.6) are solved by the ansatz

$$f_0=\frac{\sqrt{2}}{-t}+f_0^{(2)}+\cdots\,, \tag{4.9}$$

$$g_k=\epsilon(k)2\sqrt{-\tau}K_{i\omega}(-\tau)+g_k^{(3)}+\cdots\quad(k\neq0)\,, \tag{4.10}$$

$$f_k=f_k^{(2)}+\cdots\quad(k\neq0)\,, \tag{4.11}$$

$$g_0=g_0^{(3)}+\cdots\,, \tag{4.12}$$

where the superscript indicates the order of smallness ϵ. By inserting this ansatz into (4.6) and (4.7) we obtain inhomogeneous equations for $f_k^{(2)}$, $g_k^{(3)}$, etc. They can be solved, since we have analytic solutions of the corresponding homogeneous equations and thus can construct Green's functions with the correct asymptotic behavior. Rather than describing these calculations in detail, we only discuss a simplified model which contains the essential features. It consists of the two equations

$$\frac{d^2}{dt^2}f=f^3-2fg^2\,, \tag{4.13}$$

$$\left[\frac{d^2}{dt^2}-\frac{k^2}{4}\right]g=3g^3-f^2g\,. \tag{4.14}$$

With

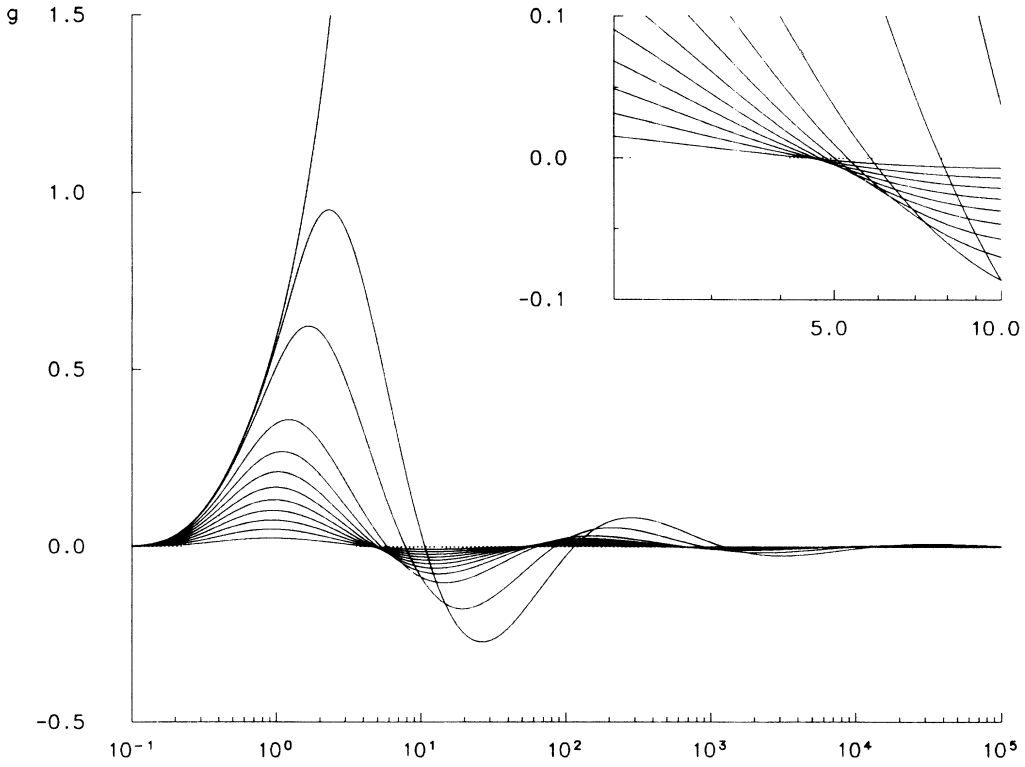

FIG. 1. Behavior of the function g vs f in the two-component model for different initial values. Upper-right corner: Enlargement showing the shift of intersection points and the formation of caustics.

$$f^{(0)}=\frac{\sqrt{2}}{(-t)} , \tag{4.15}$$

$$g^{(1)}=2\epsilon\sqrt{-\tau}K_{i\omega}(-\tau) , \tag{4.16}$$

we have the equations for $f^{(2)}$ and $g^{(3)}$

$$\left[\frac{d^2}{dt^2}-3f^{(0)2}\right]f^{(2)}=-2f^{(0)}g^{(1)2} , \tag{4.17}$$

$$\left[\frac{d^2}{dt^2}-\left[\frac{k^2}{4}-f^{(0)2}\right]\right]g^{(3)}=3g^{(1)3}-2f^{(0)}f^{(2)}g^{(1)} . \tag{4.18}$$

With the Green's functions which are given in the Appendix we first find $f^{(2)}$ as an integral involving powers of t and Bessel functions. Inserting this into the right-hand side of (4.18), we obtain an expression for $g^{(3)}$ which involves single and double integrals over Bessel functions and powers of t. Since we are mainly interested in the asymptotic behavior for $\tau\rightarrow 0$, we only present the leading behavior for small τ

$$f^{(2)}\approx\frac{\epsilon^2}{k}(-\tau/2)^2(A_0+A_2\cos\Phi+B_2\sin\Phi) , \tag{4.19}$$

$$g^{(3)}\approx\frac{\epsilon^3}{k^2}\sqrt{-\tau}[C_0\cos\Phi+C_1\sin\Phi +(-\tau)^3(A_3\cos 3\Phi+B_3\sin 3\Phi)] , \tag{4.20}$$

where the constants A,B,C are explained in the Appendix and

$$\Phi=\omega\ln\left[-\frac{\tau}{2}\right]-\phi_0 . \tag{4.21}$$

We have also studied the behavior of the set of equations (4.13) and (4.14) numerically. Figure 1 shows g versus f for a range of ϵ's, where the asymptotic form of $g^{(1)}$ [Eq. (4.16)] has been used to parametrize the starting values. Let us start with infinitesimally small values of ϵ. Initially, i.e., for $\tau\rightarrow-\infty$ or f close to zero, g grows exponentially and then turns into a decaying oscillation around the parent trajectory $f^{(0)}$. Each intersection between f and g defines a focal point. From Eqs. (4.15) for $f^{(0)}$ and (3.31) for the limiting behavior of the modified Bessel function $K_{i\omega}$ as τ tends to zero, one immediately obtains the time and the value of f at the nth intersection point of g and f to lowest order in ϵ

$$(-\tau_n/2)=\exp\left[\frac{(-n+\frac{1}{2})\pi+\phi}{\omega}\right] ,$$
$$f(t_n)=\frac{k\sqrt{2}}{-2\tau_n} . \tag{4.22}$$

This implies that the ratio of the values of f at two consecutive intersection points is constant to lowest order in ϵ (cf. Fig. 1).

When ϵ increases, each intersection point shifts to larger values of f. This leads to the formation of caustics, namely, the envelope of the trajectories to the right

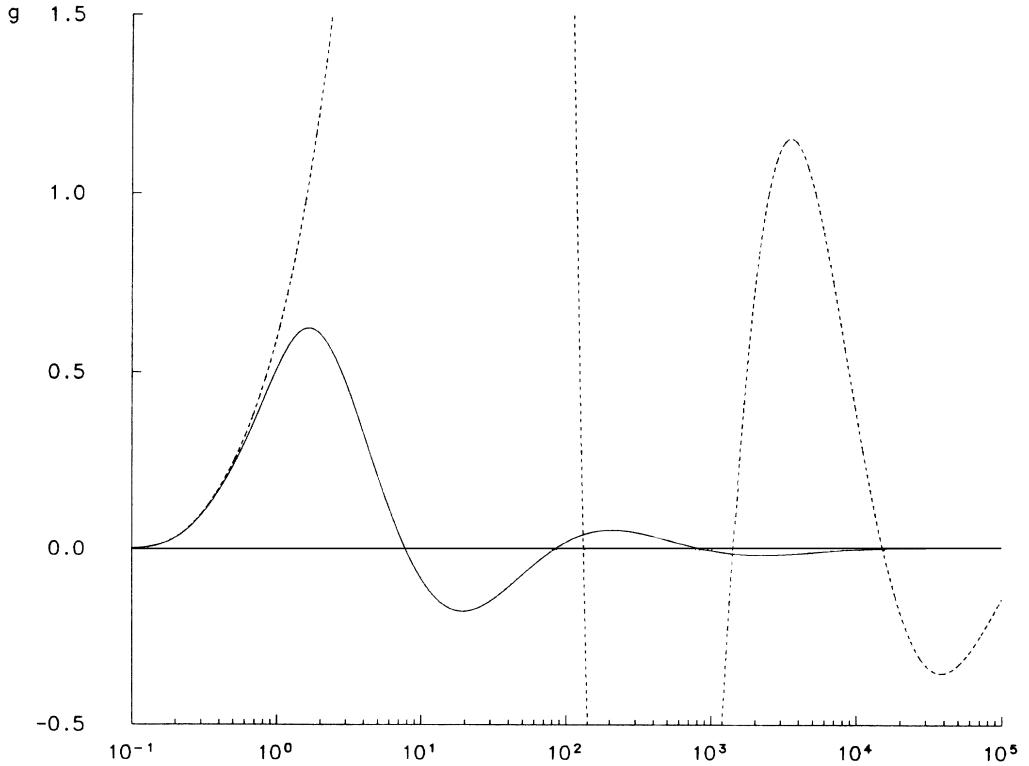

FIG. 2. The function g vs f for two initial values: Small ϵ (solid line) and ϵ close to ϵ_{cr} (dashed line).

of the focal point. This situation is illustrated in the upper-right corner of Fig. 1. To obtain this shift $\delta_n f$ analytically one has to compute to order ϵ^2. Using the asymptotic form of the higher-order corrections (4.19) and (4.20) (which we interpret as the first terms in a Fourier expansion with time-dependent coefficients A_n, B_n, C_n, and argument ϕ) we obtain

$$\delta_n f = \frac{\epsilon^2}{k(-\tau_n/2)}[C_2 + O((-\tau_n)^2)] \ . \tag{4.23}$$

The numerical result for the coefficient in the brackets is in good agreement with the analytic value for C_2 given in Eq. (A25) since the $O((-\tau_n)^2)$ corrections vanish rapidly as n gets large. With further increasing ϵ the amplitude of oscillation grows until for some ϵ_{cr} the trajectory asymptotically approaches a line $g = af + b$ with slope $a = \sqrt{2/5}$. For even larger values of ϵ the curve finally turns over, and f stars oscillating around the g axis.

In Fig. 2 we compare a trajectory with a moderate starting value (drawn curve) to one with ϵ close to ϵ_{cr} (dashed curve). It can be seen that the intersection points of the latter are shifted to rather large values of f and that the first of them lies even beyond the second intersection point of the trajectory with smaller ϵ. Hence, the larger the initial amplitude the smaller is the number of oscillations to the left of any value of f. In this sense the frequency of the oscillations depends on the initial amplitude.

Returning to the full set of equations (4.6) and (4.7), we shall not present here those results which are the analogs of (4.19) and (4.20). They are obtained by exactly the same methods, and they are of the same form as (4.19) and (4.20). As to the zeros of the g_k we again find a shift (in $f_0^{(0)}$ or in time), but this shift now depends upon all the amplitudes $\epsilon(k)$. In addition, there is no new feature which was not present in the simple two-component model: the zeros of the g_k's are no longer intersection points of our parent trajectory (2.10) [or (4.2)] and the daughters (which are described by the set $\{f_k, g_k | k \neq 0\}$). This is because to order ϵ^2, the f_k's are no longer zero, and they do not vanish at or near a zero of $g_k^{(1)}$. In order to have an intersection point, we have to slightly shift the parent trajectory, namely, to give it small (of order ϵ^2) components f_k. This seems very natural. When $\epsilon(k)$ increases, the intersection point moves away from the original parent trajectory, indicating that the caustic extends away from the focal point on the parent trajectory (2.10).

Our analytical calculations (perturbation theory) do not allow us to go very far away from the parent trajectory (2.10), but the computer analysis (Fig. 2) shows the beginning of a very interesting structure. Once the frequencies of oscillating modes start to depend upon the amplitudes, resonance between different modes become possible (i.e., there exist oscillating solutions for which the frequencies of different k modes are multiples of each other). Studies of nonlinear periodic motion show, quite in general, that in the vicinity of resonances one often encounters a rich structure of secondary resonances. Such "oscillations around oscillations" then will generate new focal points and caustics, making the cobweb of caustics denser and denser. In a future paper we shall investigate this resonance structure using somewhat different methods.

Having seen that higher-order corrections to the oscillating modes show the onset of a very promising structure, we have also to look into the other directions in the vicinity of the parent trajectory [cases (3) and (4) of Sec. III]. The latter one involves solutions which for small τ diverge away from the parent trajectory and, within our perturbative treatment, they are not promising candidates. The former case, however, leads to solutions which have the same small-τ behavior as our parent trajectory and thus have to be studied. First we use again perturbation theory and we make the ansatz

$$X_{\mathbf{k}} = X_{\mathbf{k}}^{(1)} + X_{\mathbf{k}}^{(2)} + \cdots \ . \tag{4.24}$$

In our matrix notion (4.1) the lowest-order terms is (in the limit $\tau \to 0$)

$$X_{\mathbf{k}}^{(1)}(t) \approx \frac{1}{-\tau} \begin{pmatrix} 0 & 0 & -\dfrac{-iC_{\mathbf{k}}^{(2)}}{\sqrt{2}} \\ 0 & 0 & -\dfrac{iC_{\mathbf{k}}^{(1)}}{\sqrt{2}} \\ C_{\mathbf{k}}^{(1)} & C_{\mathbf{k}}^{(2)} & 0 \end{pmatrix} \tag{4.25}$$

with arbitrary complex constants $C^{(1)}$ and $C^{(2)}$. Rather than now presenting details of calculations of higher-order corrections (the method is the same as before), we only briefly describe the results. Up to the order $n=5$ we have verified that $X^{(n)}$ vanishes for odd n, whereas for even n it has the form

$$X_{\mathbf{k}}^{(n)} \approx \frac{1}{-\tau} \begin{pmatrix} f_{11}^{(n)} & f_{12}^{(n)} & 0 \\ f_{12}^{(n)} & f_{22}^{(n)} & 0 \\ 0 & 0 & f_{33}^{(n)} \end{pmatrix} \tag{4.26}$$

(the $f_{ij}^{(n)}$ are homogeneous polynomials in $C_{\mathbf{k}'}^{(1)}$ and $C_{\mathbf{k}'}^{(2)}$ of degree n; different values of momentum $\mathbf{k}$ are now coupled together). In particular, it follows from this result (4.26) that there is no resonance; i.e., there is no change in the power of τ, and the parent trajectory (2.10) does not change significantly.

It is useful to derive this result in a different way. One notices that by disregarding in the differential equations (3.1) the first two terms A and B one has eliminated the dependence upon momentum $\mathbf{k}$, i.e., all spatial derivatives. Thus, in this approximation, the equations of motion are local and can be solved separately for each site $\mathbf{l}$. Returning to (2.9) and undoing the Fourier transformation (2.8), and using a 3×3 matrix notation analogous to (4.1), the equations that we want to solve take the form

$$\frac{d^2}{dt^2} X_{\mathbf{l}} = [X_{\mathbf{l}} \operatorname{tr}(X_{\mathbf{l}}^T X_{\mathbf{l}}) - X_{\mathbf{l}} X_{\mathbf{l}}^T X_{\mathbf{l}}] \tag{4.27}$$

(for each site $\mathbf{l}$). These equations have two kinds of O(3) symmetry: global gauge symmetry (matrix multiplication from the left) and rotations in ordinary space (matrix multiplication from the right). We are looking for solu-

tions of the form

$$X=\frac{\sqrt{2}}{-t}M=\frac{\sqrt{2}}{-t}\begin{bmatrix} m_{11} & m_{12} & m_{13} \\ m_{21} & m_{22} & m_{23} \\ m_{31} & m_{32} & m_{33} \end{bmatrix}, \tag{4.28}$$

where the m_{ij} are constants, and we have suppressed the subscript 1. The matrix M then satisfies

$$0=M-M\,\mathrm{tr}(M^TM)-MM^TM\ , \tag{4.29}$$

and it should be a generalization of our previous parent trajectory (2.10)

$$A_d=\begin{bmatrix} 1 & 0 & 0 \\ 0 & 1 & 0 \\ 0 & 0 & 0 \end{bmatrix}. \tag{4.30}$$

Because of the O(3)×O(3) symmetry, any matrix M which has the same form

$$M=R_L\,A_d R_R \tag{4.31}$$

is a solution of (4.27) [where R_L and R_R are O(3) matrices]. Writing $R_L=R_{L12}R_{L13}R'_{L12}$ and $R_R=R_{R12}R_{R13}R'_{R12}$ (with R_{ij} denoting a rotation in the i-j plane), we see that (4.31) generates a five-parameter family of solutions. On the other hand, this is already the most general solution of (4.27) that we can have. Multiply (4.29) by M^T from the left and set $B=M^TM$

$$0=B[B-\mathbb{1}(1-\mathrm{Tr}B)]\ . \tag{4.32}$$

Then either $\det B=0$, or the square brackets has to vanish. The latter case means that $B=\frac{1}{4}\mathbb{1}$ which is too far away from (4.30). Therefore, $\det B=0$, and also $\det M=0$, from which it follows that the column vectors of M are linearly dependent and lie in a plane. Hence it is possible, by successive O(3) matrix multiplications from the left or from the right, to cast M into the form

$$M\to\tilde{M}=\begin{bmatrix} \alpha & \beta & 0 \\ \gamma & \delta & 0 \\ 0 & 0 & 0 \end{bmatrix}. \tag{4.33}$$

Equation (4.29) with $M\to\tilde{M}$ then implies that $\alpha=\delta=\cos\theta$, $\beta=-\gamma=\sin\theta$ with some θ.

This result then means that in the vicinity of our parent trajectory (4.2) there exists, for each site **l**, a five-parameter set of solutions which are either gauge or space rotations of (4.2). Since these parameters can be chosen independently for each **l**, these configurations can have a rather arbitrary **l** dependence. The counting of parameters matches with our discussion in **k** space [cf. the discussion after (4.25)]. For each **k** we had started with a two-parameter set of solutions. However, solutions which go like $1/\tau$ can also be simply gauge images of our parent trajectory [(3.37)–(3.39)]. This gives us three more parameters and, again, adds up to five. By this we have a complete picture of the neighborhood of our parent trajectory (4.2), going in the direction of either gauge transformations or of the lines 3,8 or 6,7 in our nine-component vector X.

Finally let us give the parent trajectory (2.10) a small component of the form (4.25) and ask, whether the oscillating neighboring trajectories still have the same behavior as in (3.11). The answer follows immediately from our previous observation. All trajectories of the form (4.28) are obtained from (2.10) either by a spatial rotation or by a gauge transformation, and both of them leave leading-($\tau\to 0$) behavior invariant. This is because they do not change the eigenvalues of C, which are responsible for the oscillating behavior. We, therefore, conclude that the structure of oscillations will not be changed, if our parent trajectory moves into the direction of (4.25). This implies, in particular, that there are many more trajectories which are surrounded by oscillating neighbors. Which one finally will be the most important one, cannot be decided yet.

V. DISCUSSIONS

In this paper we have continued our semiclassical analysis of the weak-coupling limit of SU(2) Yang-Mills theories. Our main attention was devoted to the search for caustics: We have collected further evidence that in Yang-Mills theories there exists a dense "cobweb" of caustics which begins already in the region of very small fields. This gives further support to our expectation that caustics play an important role in the dynamics of these theories.

The source of these caustics are oscillations of classical trajectories around each other. For a particularly simple example of a "parent" trajectory we have studied, first in the linear approximation, how neighboring "daughter" trajectories oscillate around it. Each intersection between neighboring trajectories produces a focal point, which gives rise to strong quantum fluctuations and, hence, to an enhancement in the ground-state wave function. Higher-order corrections to the linear approximation indicate the onset of a rich resonance structure which makes the cobweb of caustics even more dense. This indicates that the density of caustics may eventually become so high that the enhancement resulting from the quantum fluctuations can compete with the exponential fall off of the action integral in the semiclassical wave function. Our calculations have also shown that there are many more (potentially even more important) "parent" trajectories which are also surrounded by oscillating neighbors.

This seems to suggest a new quantum-mechanical mechanism which is completely different from previous attempts of analyzing quantum field theories in the semiclassical approximation. Rather than studying single field configurations with finite action (e.g., instantons) in a dilute-gas approximation it may be more appropriate to search for regions in the space of field configurations where classical solutions stay close to each other for long times, intersect with each other, and thus produce strong quantum fluctuations. These regions may be more significant than the isolated field configurations which have been studied previously. Our analysis shows that such regions exist in Yang-Mills theories.

It then becomes mandatory to investigate the structure

of these "condensates" of classical solutions, in particular to search for some "simple" pattern. The oscillations which we have encountered in our analysis are, in our opinion, promising candidates where such an investigation could start, and we will do this as the next step of our program. In order to study these oscillations beyond the linear approximation which we have used in this paper we have to somewhat generalize our framework. So far our parent trajectory was restricted to have strictly zero energy. As a result, it takes infinite time to leave the origin and to reach the end point. If, on the other hand, we allow for a small negative energy, this trajectory will start to swing very slowly between its previous starting and end points, while its neighbors are oscillating around it. As we explained before, we then expect resonances between these oscillating modes, which will generate more caustics and thus further enhance the significance of these classical solutions. In analyzing this pattern of oscillations the observations made in Ref. 14 may be helpful. There it has been shown that certain solutions to the equations of motion of a classical (lattice) field theory follow very much the behavior predicted by the renormalization-group equations of the quantum field theory.

We have outlined in the Introduction how the structure of oscillations in the flow of classical solutions may propagate into the quantum system, namely through the caustics which generate a g^2-dependent peaking structure in the ground-state wave function. If our picture is correct, we predict that a similar g^2 dependence will also appear when one calculates expectation values of observables. In this way the small-g^2 behavior of physical quantities is closely connected with the structure of classical solutions.

ACKNOWLEDGMENTS

Most of this work was done while two of us had been visiting the CERN Theory Division. We wish to express our gratitude to John Ellis and Maurice Jacob for making this visit possible and to the Theory Division for their hospitality. One of us (J.B.) also gratefully acknowledges the hospitality of the Institute of Nonlinear Science at the University of California, San Diego, and the financial support of the Deutsche Forschungsgemeinschaft. The work of B.R. was supported in part by a Doktorandenstipendium der Universität Hamburg. The work of T.T.W. was supported in part by the United States Department of Energy under Grant No. DE-FG-02-84ER40158.

APPENDIX: HIGHER-ORDER PERTURBATION THEORY

In this appendix we give a few details of the higher-order calculations of the two-component model of Sec. IV. The equations of motion we want to solve are

$$\frac{d^2}{dt^2}f = f^3 - 2fg^2 , \tag{A1}$$

$$\left[\frac{d^2}{dt^2} - \frac{k^2}{4}\right]g = 3g^3 - f^2 g . \tag{A2}$$

We make the ansatz

$$f = \frac{\sqrt{2}}{(-t)} + f^{(2)} + \cdots , \tag{A3}$$

$$g = 2\epsilon\sqrt{-\tau}K_{i\omega}(-\tau) + g^{(3)} + \cdots . \tag{A4}$$

Inserting this ansatz into Eq. (A1) we first obtain an inhomogeneous equation for $f^{(2)}$

$$\left[\frac{d^2}{dt^2} - 3f^{(0)2}\right]f^{(2)} = -2f^{(0)}g^{(1)2} . \tag{A5}$$

With the Green's function

$$G(t,t') = \begin{cases} \frac{1}{5}t'^3 t^{-2}, & t < t' < 0 \\ \frac{1}{5}t^3 t'^{-2}, & t' < t < 0 \end{cases} \tag{A6}$$

the solution is found to be

$$f^{(2)}(t) = \frac{t^3}{5}\int_{-\infty}^{t} dt' t'^{-2}[-2f^{(0)}(t')g^{(1)2}(\tau')] + \frac{t^{-2}}{5}\int_{t}^{0} dt' t'^3[-2f^{(0)}(t')g^{(1)2}(\tau')] \tag{A7}$$

with $\tau' = kt'/2$. The Green's functions has been chosen such that for both $t \to -\infty$ and $t \to 0$, $f^{(2)}$ goes to zero. For $t \to -\infty$ the second term in (A7) dominates and goes as t^{-2}, whereas for $t \to 0$ both terms are of the same order and behave as

$$f^{(2)} \approx \frac{\epsilon^2}{k}\left[-\frac{\tau}{2}\right]^2 (A_0 + A_2\cos 2\Phi + B_2\sin 2\Phi) \tag{A8}$$

with

$$A_0 = \frac{\rho^2}{\sqrt{2}}16 \approx 0.842 , \tag{A9}$$

$$A_2 = \frac{\rho^2}{\sqrt{2}}\frac{88}{23} \approx 0.201 , \tag{A10}$$

$$B_2 = -\frac{\rho^2}{\sqrt{2}}\sqrt{7}\tfrac{24}{23} \approx -0.145 , \tag{A11}$$

$$\Phi = \omega \ln\left[-\frac{\tau}{2}\right] - \phi_0 . \tag{A12}$$

Next we consider the inhomogeneous equation for $g^{(3)}$

$$\left[\frac{d^2}{dt^2} - \left[\frac{k^2}{4} - f^{(0)2}\right]\right]g^{(3)} = 3g^{(1)3} - 2f^{(0)}f^{(2)}g^{(1)} . \tag{A13}$$

The Green's function is given by

$$G(\tau,\tau')=\begin{cases}0, & \tau<\tau'<0\ , \\ \dfrac{u_2(\tau)u_1(\tau')-u_1(\tau)u_2(\tau')}{w}, & \tau'<\tau<0\ ,\end{cases} \tag{A14}$$

where $\tau=kt/2$, $\nu=i\omega=i\sqrt{7}/2$, and

$$u_1(\tau)=\mathrm{Re}\left[i\pi\exp\frac{i\pi\nu}{2}\sqrt{-\tau}H_\nu^{(1)}(-i\tau)\right]=2\sqrt{-\tau}K_{i\omega}(-\tau)\ , \tag{A15}$$

$$u_2(\tau)=\mathrm{Re}\left[\pi\exp-\frac{i\pi\nu}{2}\sqrt{-\tau}H_\nu^{(2)}(-i\tau)\right]=2\pi\sqrt{-\tau}\,\mathrm{Re}I_{i\omega}(-\tau)\ , \tag{A16}$$

$$W=u_2'u_1-u_1'u_2=-4\pi\ . \tag{A17}$$

With this Green's function $g^{(3)}$ goes as $e^\tau/(-\tau)^2$ for $-\tau\to\infty$, whereas for small τ the leading behavior is found to be

$$g^{(3)}\approx\frac{\epsilon^3}{k^2}\sqrt{-\tau}\{[C_0+O((-\tau)^2)]\cos\Phi+[C_1+O((-\tau)^2)]\sin\Phi+(-\tau)^3(A_3\cos3\Phi+B_3\sin3\Phi)\} \tag{A18}$$

with

$$C_0=32\rho\int_0^\infty dz\left[3z^2\mathrm{Re}I_\nu(z)K_\nu^3(z)-\tfrac{8}{5}z^{-2}\mathrm{Re}I_\nu(z)K_\nu(z)\int_0^z dz'z'^3K_\nu^2(z')-\tfrac{8}{5}z^{-2}K_\nu^2(z)\int_0^z dz'z'^3\mathrm{Re}I_\nu(z')K_\nu(z')\right]\ , \tag{A19}$$

$$C_1=-\frac{32}{\omega\rho}\int_0^\infty dz\left[3z^2K_\nu^4(z)-\tfrac{16}{5}z^{-2}K_\nu^2(z)\int_0^z dz'z'^3K_\nu^2(z')\right] \tag{A20}$$

$$=-\frac{32}{\omega\rho}\int_0^\infty dz\left\{3z^2K_\nu^4(z)-\tfrac{16}{15}\left[\frac{K_\nu^2(\nu^2-1)\nu^2\rho^2}{z^2}+K_\nu^2K_\nu'^2\left[\nu^2-1-\frac{z^2}{2}\right]+K_\nu^4\left[-\frac{1+2\nu^2}{4}+\frac{z^2}{2}+\frac{\nu^2(1-\nu^2)}{z^2}\right]\right]\right\}$$

$$\approx-0.40\ , \tag{A21}$$

$$A_3=\frac{16\rho^3}{\omega}\sqrt{7}[\tfrac{1}{16}(-\tfrac{17}{20}+\tfrac{14}{115})+\tfrac{1}{37}(\tfrac{31}{20}-\tfrac{22}{115})]\approx-0.005\,72\ , \tag{A22}$$

$$B_3=\frac{16\rho^3}{\omega}[\tfrac{1}{16}(\tfrac{7}{4}-\tfrac{2}{23})+\tfrac{1}{37}(-\tfrac{7}{5}-\tfrac{4}{115})]\approx0.0160\ . \tag{A23}$$

From (A3), (A8), and (A4), (A18) we compute the shift of the nth zero of $g(\tau)$

$$\delta f=\frac{\epsilon^2}{k(-\tau_n/2)}[C_2+O((-\tau_n)^2)] \tag{A24}$$

with

$$C_2=-\frac{\sqrt{2}}{8\omega\rho}C_1\quad\approx0.196\ . \tag{A25}$$

The coefficient C_2 is positive; i.e., the zeros move towards larger values of f as ϵ increases.

[1]J. Bartels and T. T. Wu, Phys. Rev. D **37**, 2307 (1988).

[2]C. N. Yang and R. L. Mills, Phys. Rev. **96**, 191 (1954).

[3]G. S. Matinyan, G. K. Savvidy, and N. G. Ter-Arutyunyan-Savvidy, Zh. Eksp. Teor. Fiz. **80**, 830 (1981) [Sov. Phys. JETP **53**, 421 (1981)].

[4]B. V. Chirikov and D. L. Shepelyanskij, Pis'ma Zh. Eksp. Teor. Fiz. **34**, 171 (1981) [JETP Lett. **34**, 163 (1981)].

[5]G. S. Matinyan, G. K. Savvidy, and N. G. Ter-Arutyunyan-Savvidy, Pis'ma Zh. Eksp. Teor. Fiz. **34**, 613 (1981) [JETP Lett. **34**, 590 (1981)].

[6]E. S. Nikolaevskij and L. N. Shur, Pis'ma Zh. Eksp. Teor. Fiz. **36**, 176 (1982) [JETP Lett. **36**, 218 (1981)].

[7]M. Lüscher and G. Münster, Nucl. Phys. **B232**, 445 (1984).

[8]J. Bartels and T. T. Wu, Z. Phys. C **33**, 583 (1987).

[9]M. V. Berry, in *Chaotic Behavior of Deterministic Systems,* proceedings of the Les Houches Summer School, Les Houches, France, 1981, edited by G. Iooss, H. G. Helleman, and R. Stora (Les Houches Summer School Proceedings, Vol. 36) (North-Holland, Amsterdam, 1983).

[10]M. V. Berry, N. L. Balazs, M. Tabor, and A. Voros, Ann. Phys. (N.Y.) **122**, 26 (1979).

[11]H. J. Korsch and M. V. Berry, Physica Utrecht **3D**, 627 (1981).

[12]A. A. Belavin, A. M. Polyakov, A. S. Schwartz, and Yu. S. Tyupkin, Phys. Lett. **59B**, 85 (1975).

[13]A. Actor, Rev. Mod. Phys. **51**, 461 (1979).

[14]J. Bartels and S.-J. Chang, Phys. Rev. A **41**, 598 (1990).